Solving Einstein's Equations for Binary Black Hole Spacetimes

Lee Lindblom

Theoretical Astrophysics, Caltech

MESGW 2010, São Sebastião, Brazil
30 November 2010

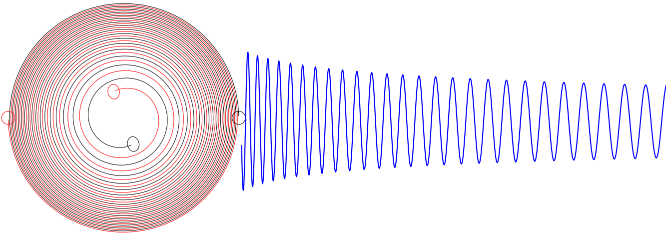

History of Numerical Solution of the BBH Problem:

- First Axisymmetric Head-On — Hahn & Lindquist (1964).
- Better Axisymmetric Head-On — Eppley & Smarr (1975-77).
- Good Axisymmetric Head-On — NCSA group (1993-94).

History of Numerical Solution of the BBH Problem:

- First Axisymmetric Head-On — Hahn & Lindquist (1964).
- Better Axisymmetric Head-On — Eppley & Smarr (1975-77).
- Good Axisymmetric Head-On — NCSA group (1993-94).
- Full 3D one orbit, no merger – Penn State group (2003-04).

History of Numerical Solution of the BBH Problem:

- First Axisymmetric Head-On — Hahn & Lindquist (1964).
- Better Axisymmetric Head-On — Eppley & Smarr (1975-77).
- Good Axisymmetric Head-On — NCSA group (1993-94).
- Full 3D one orbit, no merger – Penn State group (2003-04).
- First full inspiral + merger + ringdown – Pretorius (2005).

History of Numerical Solution of the BBH Problem:

- First Axisymmetric Head-On — Hahn & Lindquist (1964).
- Better Axisymmetric Head-On — Eppley & Smarr (1975-77).
- Good Axisymmetric Head-On — NCSA group (1993-94).
- Full 3D one orbit, no merger – Penn State group (2003-04).
- First full inspiral + merger + ringdown – Pretorius (2005).
- Moving puncture method – Brownsville + Goddard (2005).

History of Numerical Solution of the BBH Problem:

- First Axisymmetric Head-On — Hahn & Lindquist (1964).
- Better Axisymmetric Head-On — Eppley & Smarr (1975-77).
- Good Axisymmetric Head-On — NCSA group (1993-94).
- Full 3D one orbit, no merger – Penn State group (2003-04).
- First full inspiral + merger + ringdown – Pretorius (2005).
- Moving puncture method – Brownsville + Goddard (2005).
- Unequal masses – Goddard + Penn State groups (2006).
- Non-zero spins – Brownsville + AEI (2006-07).
- Post merger recoils (up to $\sim$ 4000 km/s)
  – Jena + AEI + Rochester (2007).
- Large mass ratios (1:10) – Jena (2009).
- Generic spins with precession – Rochester (2009).
- High precision inspiral + merger + ringdown waveforms
  – AEI + Caltech/Cornell (2009).
- Very large mass ratios (1:100) – Rochester (2010).
- Very high spins ($\chi \approx 0.95$) – Caltech/Cornell (2010).

Outline of Talk:

- Fundamental Einstein Equations Issues.
  - Specifying the Gauge in Einstein's Equations.
  - Making Einstein's Equations Hyperbolic.
  - Constraints and Constraint Damping.
  - "Good" Gauge Conditions for Binary Black Holes.
- Numerical Method Issues.
  - Solving Evolution Equations.
  - Horizon Tracking Coordinates.
  - Dual-Frame Evolution.
  - Horizon Distortion Maps.
  - Spectral AMR.
- A Sample of Recent BBH Evolution Results.
  - Post-Merger Recoils.
  - Accurate Long Waveforms.
  - Very High Mass Ratios.
  - Very High Spins.

Traditional ADM Gauge Conditions

- Construct a foliation of spacetime by spatial slices.
- Choose a time function with t = const. on these slices.
- Choose spatial coordinates, x^k, on each slice.

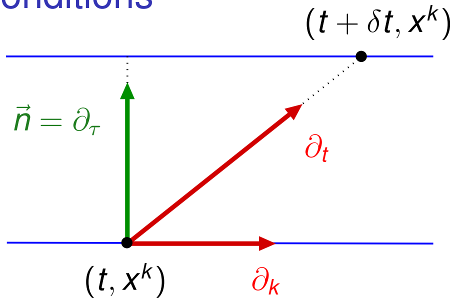

- Decompose the 4-metric ψ_{ab} into its 3+1 parts:
  $ds^2 = \psi_{ab}dx^a dx^b = -N^2 dt^2 + g_{ij}(dx^i + N^i dt)(dx^j + N^j dt)$.
- The lapse N and shift N^i measure how coordinates are laid out on spacetime:

$$\vec{n} = \partial_\tau = \frac{\partial x^a}{\partial \tau}\partial_a = \frac{\partial t}{\partial \tau}\partial_t + \frac{\partial x^k}{\partial \tau}\partial_k,$$

$$= \frac{1}{N}\partial_t - \frac{N^k}{N}\partial_k.$$

- Spacetime coordinates are determined in the traditional ADM method by specifying the lapse N and shift N^i.

ADM Evolution System

- When the gauge is determined by specifying the lapse N and shift N^k, the Einstein equations becomes a set of evolution equations for the spatial metric g_{ij} and extrinsic curvature K_{ij}:

$$\begin{aligned}\partial_t g_{ij} &= -2NK_{ij} + E_{ij}(g, N, \partial_x g, \partial_x N),\\ \partial_t K_{ij} &= F_{ij}(g, K, N, \partial_x g, \partial_x K, \partial_x N, \partial_x\partial_x g, \partial_x\partial_x N).\end{aligned}$$

- The Einstein equations also include constraints:

$$\begin{aligned}0 &= \mathcal{M}_t \equiv \mathcal{M}_t(g, K, \partial_x g, \partial_x\partial_x g),\\ 0 &= \mathcal{M}_i \equiv \mathcal{M}_i(g, K, \partial_x g, \partial_x K).\end{aligned}$$

- Einstein's equations do not determine the time derivatives of the lapse N and shift N^i.
- This traditional form of the Einstein equations is not hyperbolic, and numerical solutions are non-convergent.

Generalized Harmonic Gauge Conditions

- An alternate way to specify the gauge (i.e. coordinates) in the Einstein equations is through the gauge source function H^a:
- Let H^a denote the function obtained by the action of the covariant scalar wave operator on the coordinates x^a:

$$H^a \equiv \nabla^c\nabla_c x^a \;=\; \psi^{bc}(\partial_b\partial_c x^a - \Gamma^e_{bc}\partial_e x^a) = -\Gamma^a,$$

where $\Gamma^a = \psi^{bc}\Gamma^a{}_{bc}$ and ψ_{ab} is the 4-metric.

Generalized Harmonic Gauge Conditions

- An alternate way to specify the gauge (i.e. coordinates) in the Einstein equations is through the gauge source function H^a:
- Let H^a denote the function obtained by the action of the covariant scalar wave operator on the coordinates x^a:

$$H^a \equiv \nabla^c \nabla_c x^a \;=\; \psi^{bc}(\partial_b \partial_c x^a - \Gamma^e_{bc} \partial_e x^a) = -\Gamma^a,$$

  where $\Gamma^a = \psi^{bc} \Gamma^a{}_{bc}$ and ψ_{ab} is the 4-metric.

- Specifying coordinates by the *generalized harmonic* (GH) method can be accomplished by choosing a gauge-source function $H^a(x, \psi)$, e.g. $H^a = \psi^{ab} H_b(x)$, and requiring that

$$H^a(x, \psi) = -\Gamma^a = \partial_b \left(\sqrt{-\psi}\psi^{ab} \right) / \sqrt{-\psi}.$$

Einstein's Equation with the GH Method

- The spacetime Ricci tensor can be written as:

$$R_{ab} \;=\; -\tfrac{1}{2}\psi^{cd}\partial_c\partial_d\psi_{ab} + \nabla_{(a}\Gamma_{b)} + F_{ab}(\psi,\partial\psi),$$

  where ψ_{ab} is the 4-metric, and $\Gamma_a = \psi^{bc}\Gamma_{abc}$.

- The Generalized Harmonic Einstein equation is obtained by replacing Γ_a with $-H_a(x,\psi) = -\psi_{ab}H^b(x,\psi)$:

$$R_{ab} - \nabla_{(a}\left[\Gamma_{b)} + H_{b)}\right] = -\tfrac{1}{2}\psi^{cd}\partial_c\partial_d\psi_{ab} - \nabla_{(a}H_{b)} + F_{ab}(\psi,\partial\psi).$$

- The vacuum GH Einstein equation, $R_{ab} = 0$ with $\Gamma_a + H_a = 0$, is therefore manifestly hyperbolic, having the same principal part as the scalar wave equation:

$$0 = \nabla_a\nabla^a\Phi = \psi^{ab}\partial_a\partial_b\Phi + F(\partial\Phi).$$

Gauge and Hyperbolicity in Electromagnetism

- The usual representation of the vacuum Maxwell equations split into evolution equations and constraints:

$$\partial_t \vec{E} = \vec{\nabla} \times \vec{B}, \qquad \nabla \cdot \vec{E} = 0,$$
$$\partial_t \vec{B} = -\vec{\nabla} \times \vec{E}, \qquad \nabla \cdot \vec{B} = 0.$$

  These equations are often written in the more compact 4-dimensional notation: $\nabla^a F_{ab} = 0$ and $\nabla_{[a} F_{bc]} = 0$, where F_{ab} has components $\vec{E}$ and $\vec{B}$.

Gauge and Hyperbolicity in Electromagnetism

- The usual representation of the vacuum Maxwell equations split into evolution equations and constraints:

$$\partial_t \vec{E} = \vec{\nabla} \times \vec{B}, \qquad \nabla \cdot \vec{E} = 0,$$
$$\partial_t \vec{B} = -\vec{\nabla} \times \vec{E}, \qquad \nabla \cdot \vec{B} = 0.$$

  These equations are often written in the more compact 4-dimensional notation: $\nabla^a F_{ab} = 0$ and $\nabla_{[a} F_{bc]} = 0$, where F_{ab} has components $\vec{E}$ and $\vec{B}$.
- Maxwell's equations can then be re-expressed in terms of a vector potential $F_{ab} = \nabla_a A_b - \nabla_b A_a$:

$$\nabla^a \nabla_a A_b - \nabla_b \nabla^a A_a = 0.$$

Gauge and Hyperbolicity in Electromagnetism

- The usual representation of the vacuum Maxwell equations split into evolution equations and constraints:

$$\partial_t \vec{E} = \vec{\nabla} \times \vec{B}, \qquad \nabla \cdot \vec{E} = 0,$$
$$\partial_t \vec{B} = -\vec{\nabla} \times \vec{E}, \qquad \nabla \cdot \vec{B} = 0.$$

  These equations are often written in the more compact 4-dimensional notation: $\nabla^a F_{ab} = 0$ and $\nabla_{[a} F_{bc]} = 0$, where F_{ab} has components $\vec{E}$ and $\vec{B}$.
- Maxwell's equations can then be re-expressed in terms of a vector potential $F_{ab} = \nabla_a A_b - \nabla_b A_a$:

$$\nabla^a \nabla_a A_b - \nabla_b \nabla^a A_a = 0.$$

- This form of Maxwell's equations is manifestly hyperbolic as long as the gauge is chosen correctly, e.g., let $\nabla^a A_a = H(x, t, A)$, giving:

$$\nabla^a \nabla_a A_b \equiv \left(-\partial_t^2 + \partial_x^2 + \partial_y^2 + \partial_z^2\right) A_b = \nabla_b H.$$

The Constraint Problem

- Fixing the gauge in an appropriate way makes the Einstein equations hyperbolic, so the initial value problem becomes well-posed mathematically.
- In a well-posed representation, the constraints, $\mathcal{C} = 0$, remain satisfied for all time if they are satisfied initially.

The Constraint Problem

- Fixing the gauge in an appropriate way makes the Einstein equations hyperbolic, so the initial value problem becomes well-posed mathematically.
- In a well-posed representation, the constraints, $\mathcal{C} = 0$, remain satisfied for all time if they are satisfied initially.
- There is no guarantee, however, that constraints that are “small” initially will remain “small”.
- Constraint violating instabilities were one of the major problems that made progress on binary black hole solutions so slow.
- Special representations of the Einstein equations are needed that control the growth of any constraint violations.

Constraint Damping in Electromagnetism

- Electromagnetism is described as the hyperbolic evolution equation $\nabla^a\nabla_a A_b = \nabla_b H$.
  Where have the usual $\vec{\nabla}\cdot\vec{E} = \vec{\nabla}\cdot\vec{B} = 0$ constraints gone?

Constraint Damping in Electromagnetism

- Electromagnetism is described as the hyperbolic evolution equation $\nabla^a \nabla_a A_b = \nabla_b H$.
  Where have the usual $\vec{\nabla} \cdot \vec{E} = \vec{\nabla} \cdot \vec{B} = 0$ constraints gone?
- Gauge condition becomes a constraint: $0 = \mathcal{C} \equiv \nabla^a A_a - H$.
- Maxwell's equations imply that this constraint is preserved:

$$\nabla^a \nabla_a \mathcal{C} = 0.$$

Constraint Damping in Electromagnetism

- Electromagnetism is described as the hyperbolic evolution equation $\nabla^a\nabla_a A_b = \nabla_b H$.
  Where have the usual $\vec{\nabla}\cdot\vec{E} = \vec{\nabla}\cdot\vec{B} = 0$ constraints gone?
- Gauge condition becomes a constraint: $0 = \mathcal{C} \equiv \nabla^a A_a - H$.
- Maxwell's equations imply that this constraint is preserved:

$$\nabla^a\nabla_a \mathcal{C} = 0.$$

- Modify evolution equations by adding multiples of the constraints:

$$\nabla^a\nabla_a A_b = \nabla_b H + \gamma_0 t_b \mathcal{C} = \nabla_b H + \gamma_0 t_b \left(\nabla^a A_a - H\right).$$

- These changes effect the constraint evolution equation,

$$\nabla^a\nabla_a \mathcal{C} - \gamma_0 t^b \nabla_b \mathcal{C} = 0,$$

  so constraint violations are damped when $\gamma_0 > 0$.

Generalized Harmonic Evolution System

- A similar constraint damping mechanism exists for the GH evolution system:

$$\begin{aligned} 0 &= R_{ab} - \nabla_{(a}\Gamma_{b)} - \nabla_{(a}H_{b)}, \\ &= R_{ab} - \nabla_{(a}\mathcal{C}_{b)}, \end{aligned}$$

  where $\mathcal{C}_a = H_a + \Gamma_a$. Without constraint damping, these equations are very unstable to constraint violating instabilities.

Generalized Harmonic Evolution System

- A similar constraint damping mechanism exists for the GH evolution system:

$$\begin{aligned} 0 &= R_{ab} - \nabla_{(a}\Gamma_{b)} - \nabla_{(a}H_{b)}, \\ &= R_{ab} - \nabla_{(a}\mathcal{C}_{b)}, \end{aligned}$$

 where $\mathcal{C}_a = H_a + \Gamma_a$. Without constraint damping, these equations are very unstable to constraint violating instabilities.

- Imposing coordinates using a GH gauge function profoundly changes the constraints. The GH constraint, $\mathcal{C}_a = 0$, where

$$\mathcal{C}_a = H_a + \Gamma_a,$$

 depends only on first derivatives of the metric. The standard Hamiltonian and momentum constraints, $\mathcal{M}_a = 0$, are determined by the derivatives of the gauge constraint $\mathcal{C}_a$:

$$\mathcal{M}_a \equiv \left[R_{ab} - \frac{1}{2}\psi_{ab}R\right]n^b = \left[\nabla_{(a}\mathcal{C}_{b)} - \frac{1}{2}\psi_{ab}\nabla^c\mathcal{C}_c\right]n^b.$$

Constraint Damping Generalized Harmonic System

- Pretorius (based on a suggestion from Gundlach, et al.) modified the GH system by adding terms proportional to the gauge constraints:

$$0 = R_{ab} - \nabla_{(a}\mathcal{C}_{b)} + \gamma_0 \left[n_{(a}\mathcal{C}_{b)} - \frac{1}{2}\psi_{ab}\, n^c\, \mathcal{C}_c \right],$$

  where n^a is a unit timelike vector field. Since $\mathcal{C}_a = H_a + \Gamma_a$ depends only on first derivatives of the metric, these additional terms do not change the hyperbolic structure of the system.

Constraint Damping Generalized Harmonic System

- Pretorius (based on a suggestion from Gundlach, et al.) modified the GH system by adding terms proportional to the gauge constraints:

$$0 \;=\; R_{ab} - \nabla_{(a}\mathcal{C}_{b)} + \gamma_0\left[n_{(a}\mathcal{C}_{b)} - \frac{1}{2}\psi_{ab}\, n^c\, \mathcal{C}_c\right],$$

  where n^a is a unit timelike vector field. Since $\mathcal{C}_a = H_a + \Gamma_a$ depends only on first derivatives of the metric, these additional terms do not change the hyperbolic structure of the system.
- Evolution of the constraints $\mathcal{C}_a$ follow from the Bianchi identities:

$$0 \;=\; \nabla^c\nabla_c\mathcal{C}_a - 2\gamma_0\nabla^c\left[n_{(c}\mathcal{C}_{a)}\right] + \mathcal{C}^c\nabla_{(c}\mathcal{C}_{a)} - \frac{1}{2}\gamma_0\; n_a\mathcal{C}^c\mathcal{C}_c.$$

  This is a damped wave equation for $\mathcal{C}_a$, that drives all small short-wavelength constraint violations toward zero as the system evolves (for $\gamma_0 > 0$).

Numerical Tests of the GH Evolution System

- 3D numerical evolutions of static black-hole spacetimes illustrate the constraint damping properties of the GH evolution system.
- These evolutions are stable and convergent when $\gamma_0 = \gamma_2 = 1$.

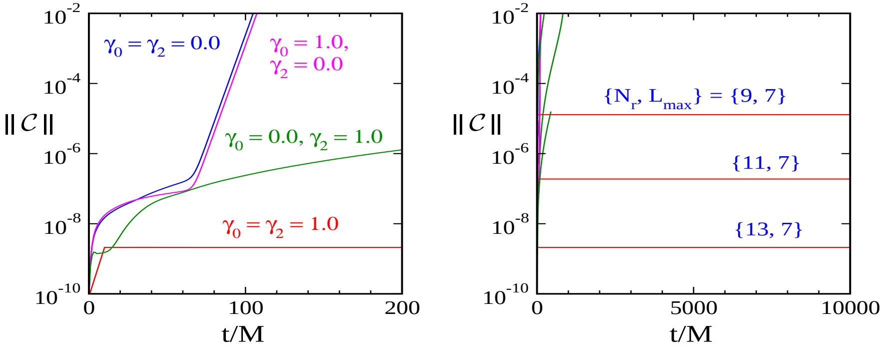

- The boundary conditions used for this simple test problem freeze the incoming characteristic fields to their initial values.

Dynamical Gauge Conditions

- The spacetime coordinates x^b are fixed in the generalized harmonic Einstein equations by specifying H^b:

$$\nabla^a\nabla_a x^b \equiv H^b.$$

- The generalized harmonic Einstein equations remain hyperbolic as long as the gauge source functions H^b are taken to be functions of the coordinates x^b and the spacetime metric ψ_{ab}.
- The simplest choice $H^b = 0$ (harmonic gauge) fails for very dynamical spacetimes, like binary black hole mergers.
- We think this failure occurs because the coordinates themselves become very dynamical solutions of the wave equation $\nabla^a\nabla_a x^b = 0$ in these situations.
- Another simple choice – keeping H^b fixed in the co-moving frame of the black holes – works well during the long inspiral phase, but fails when the black holes begin to merge.

Dynamical Gauge Conditions II

- Some of the extraneous gauge dynamics could be removed by adding a damping term to the harmonic gauge condition:

$$\nabla^a\nabla_a x^b = H^b = \mu n^a\partial_a x^b = \mu n^b = \mu\psi^{bt}/\sqrt{-\psi^{tt}}.$$

- This works well for the spatial coordinates x^i, driving them toward solutions of the spatial Laplace equation on the timescale $1/\mu$.

Dynamical Gauge Conditions II

- Some of the extraneous gauge dynamics could be removed by adding a damping term to the harmonic gauge condition:

$$\nabla^a\nabla_a x^b = H^b = \mu n^a \partial_a x^b = \mu n^b = \mu\psi^{bt}/\sqrt{-\psi^{tt}}.$$

- This works well for the spatial coordinates x^i, driving them toward solutions of the spatial Laplace equation on the timescale $1/\mu$.
- For the time coordinate t, this damped wave condition drives t to a time independent constant, which is not a good coordinate.
- A better choice sets H_t proportional to $\mu \log \sqrt{-\det g_{ij}/\psi^{tt}}$. This time coordinate condition keeps the ratio $\det g_{ij}/\psi^{tt}$ close to unity, even during binary black hole mergers where it becomes of order 100 using our simpler gauge conditions.

Outline of Talk:

- Fundamental Einstein Equation Issues.
  - How Gauge is Specified.
  - Making Einstein's Equation Hyperbolic.
  - Constraints and Constraint Damping.
  - Good Gauge Conditions.
- Numerical Method Issues.
  - Solving Evolution Equations.
  - Horizon Tracking Coordinates.
  - Dual-Frame Evolution.
  - Horizon Distortion Maps.
  - Spectral AMR.
- A Sample of Recent BBH Evolution Results.
  - Post-Merger Recoils.
  - Accurate Long Waveforms.
  - Very High Mass Ratios.
  - Very High Spins.

Numerical Solution of Evolution Equations

$$\partial_t u = F(u, \partial_x u, x, t).$$

- Choose a grid of spatial points, x_n.

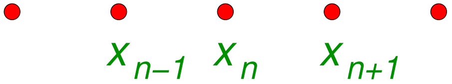

Numerical Solution of Evolution Equations

$$\partial_t u = F(u, \partial_x u, x, t).$$

- Choose a grid of spatial points, x_n.
- Evaluate the function u on this grid: $u_n(t) = u(x_n, t)$.

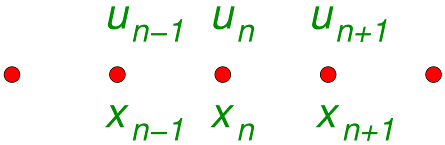

Numerical Solution of Evolution Equations

$$\partial_t u = F(u, \partial_x u, x, t).$$

- Choose a grid of spatial points, x_n.
- Evaluate the function u on this grid: $u_n(t) = u(x_n, t)$.

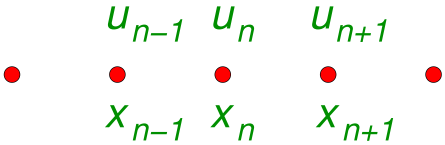

- Approximate the spatial derivatives at the grid points $\partial_x u(x_n) = \sum_k D_{nk} u_k$.

Numerical Solution of Evolution Equations

$$\partial_t u = F(u, \partial_x u, x, t).$$

- Choose a grid of spatial points, x_n.
- Evaluate the function u on this grid: $u_n(t) = u(x_n, t)$.

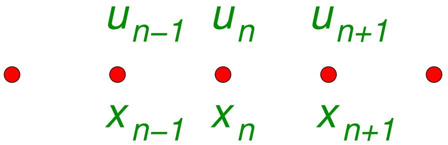

- Approximate the spatial derivatives at the grid points
  $\partial_x u(x_n) = \sum_k D_{n\,k} u_k$.
- Evaluate F at the grid points x_n in terms of the u_k: $F(u_k, x_n, t)$.

Numerical Solution of Evolution Equations

$$\partial_t u = F(u, \partial_x u, x, t).$$

- Choose a grid of spatial points, x_n.
- Evaluate the function u on this grid: $u_n(t) = u(x_n, t)$.

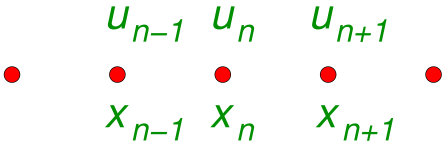

- Approximate the spatial derivatives at the grid points
  $\partial_x u(x_n) = \sum_k D_{n\,k} u_k$.
- Evaluate F at the grid points x_n in terms of the u_k: $F(u_k, x_n, t)$.
- Solve the coupled system of ordinary differential equations,

$$\frac{du_n(t)}{dt} = F[u_k(t), x_n, t],$$

using standard numerical methods (e.g. Runge-Kutta).

Basic Numerical Methods

- Different numerical methods use different ways of choosing the grid points x_n, and different expressions for the spatial derivatives $\partial_x u(x_n) = \sum_k D_{n\,k} u_k$.

Basic Numerical Methods

- Different numerical methods use different ways of choosing the grid points x_n, and different expressions for the spatial derivatives $\partial_x u(x_n) = \sum_k D_{n\,k} u_k$.
- Most numerical groups use finite difference methods:
  - Uniformly spaced grids: $x_n - x_{n-1} = \Delta x =$ constant.
  - Use Taylor expansions to obtain approximate expressions for the derivatives, e.g.,

$$\partial_x u(x_n) = \frac{u_{n+1} - u_{n-1}}{2\Delta x} + \mathcal{O}(\Delta x^2).$$

Basic Numerical Methods

- Different numerical methods use different ways of choosing the grid points x_n, and different expressions for the spatial derivatives $\partial_x u(x_n) = \sum_k D_{n\,k} u_k$.
- Most numerical groups use finite difference methods:
  - Uniformly spaced grids: $x_n - x_{n-1} = \Delta x =$ constant.
  - Use Taylor expansions to obtain approximate expressions for the derivatives, e.g.,
$$\partial_x u(x_n) = \frac{u_{n+1} - u_{n-1}}{2\Delta x} + \mathcal{O}(\Delta x^2).$$
- Grid spacing decreases as the number of grid points N increases, $\Delta x \sim 1/N$. Errors in finite difference methods scale as N^{-p}.
- Many NR groups with finite difference codes now use 6^{th} or 8^{th} order codes.

Basic Numerical Methods II

- A few groups (Caltech/Cornell, Meudon) use spectral methods.

Basic Numerical Methods II

- A few groups (Caltech/Cornell, Meudon) use spectral methods.
- Represent functions as finite sums: $u(x,t) = \sum_{k=0}^{N-1} \tilde{u}_k(t) e^{ikx}$.
- Choose grid points x_n to allow efficient (and exact) inversion of the series: $\tilde{u}_k(t) = \sum_{n=0}^{N-1} w_n\, u(x_n, t) e^{-ikx_n}$.

Basic Numerical Methods II

- A few groups (Caltech/Cornell, Meudon) use spectral methods.
- Represent functions as finite sums: $u(x,t) = \sum_{k=0}^{N-1} \tilde{u}_k(t) e^{ikx}$.
- Choose grid points x_n to allow efficient (and exact) inversion of the series: $\tilde{u}_k(t) = \sum_{n=0}^{N-1} w_n \, u(x_n, t) e^{-ikx_n}$.
- Obtain derivative formulas by differentiating the series: $\partial_x u(x_n, t) = \sum_{k=0}^{N-1} \tilde{u}_k(t) \partial_x e^{ikx_n} = \sum_{m=0}^{N-1} D_{n\,m} \, u(x_m, t)$.

Basic Numerical Methods II

- A few groups (Caltech/Cornell, Meudon) use spectral methods.
- Represent functions as finite sums: $u(x,t) = \sum_{k=0}^{N-1} \tilde{u}_k(t) e^{ikx}$.
- Choose grid points x_n to allow efficient (and exact) inversion of the series: $\tilde{u}_k(t) = \sum_{n=0}^{N-1} w_n\, u(x_n, t) e^{-ikx_n}$.
- Obtain derivative formulas by differentiating the series: $\partial_x u(x_n, t) = \sum_{k=0}^{N-1} \tilde{u}_k(t) \partial_x e^{ikx_n} = \sum_{m=0}^{N-1} D_{n\,m}\, u(x_m, t)$.
- Errors in spectral methods are dominated by the size of $\tilde{u}_N$.
- Estimate the errors (e.g. for Fourier series of *smooth* functions):

$$\begin{aligned} \tilde{u}_N &= \frac{1}{2\pi}\int_{-\pi}^{\pi} u(x) e^{-iNx} dx = \frac{1}{2\pi}\left(\frac{-i}{N}\right)\int_{-\pi}^{\pi}\frac{du(x)}{dx} e^{-iNx} dx \\ &= \frac{1}{2\pi}\left(\frac{-i}{N}\right)^p \int_{-\pi}^{\pi}\frac{d^p u(x)}{dx^p} e^{-iNx} dx \le \frac{1}{N^p}\max\left|\frac{d^p u(x)}{dx^p}\right|. \end{aligned}$$

Basic Numerical Methods II

- A few groups (Caltech/Cornell, Meudon) use spectral methods.
- Represent functions as finite sums: $u(x,t) = \sum_{k=0}^{N-1} \tilde{u}_k(t) e^{ikx}$.
- Choose grid points x_n to allow efficient (and exact) inversion of the series: $\tilde{u}_k(t) = \sum_{n=0}^{N-1} w_n\, u(x_n, t) e^{-ikx_n}$.
- Obtain derivative formulas by differentiating the series: $\partial_x u(x_n,t) = \sum_{k=0}^{N-1} \tilde{u}_k(t) \partial_x e^{ikx_n} = \sum_{m=0}^{N-1} D_{n\,m}\, u(x_m, t)$.
- Errors in spectral methods are dominated by the size of $\tilde{u}_N$.
- Estimate the errors (e.g. for Fourier series of *smooth* functions):

$$\begin{aligned}\tilde{u}_N &= \frac{1}{2\pi}\int_{-\pi}^{\pi} u(x) e^{-iNx} dx = \frac{1}{2\pi}\left(\frac{-i}{N}\right)\int_{-\pi}^{\pi}\frac{du(x)}{dx} e^{-iNx} dx \\ &= \frac{1}{2\pi}\left(\frac{-i}{N}\right)^p \int_{-\pi}^{\pi}\frac{d^p u(x)}{dx^p} e^{-iNx} dx \le \frac{1}{N^p}\max\left|\frac{d^p u(x)}{dx^p}\right|.\end{aligned}$$

- Errors in spectral methods decrease faster than any power of N.

Comparing Different Numerical Methods

- Wave propagation with second-order finite difference method:

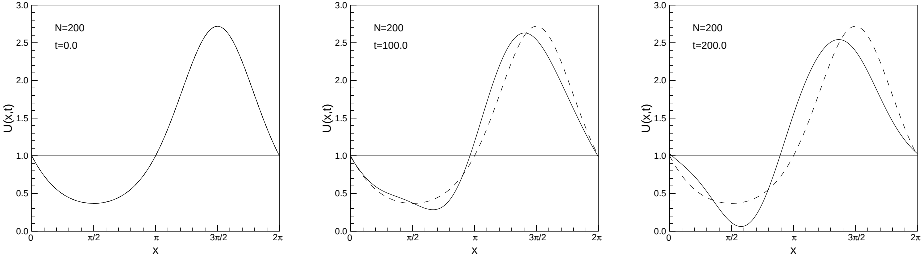

Figures from Hesthaven, Gottlieb, & Gottlieb (2007).

Comparing Different Numerical Methods

- Wave propagation with second-order finite difference method:

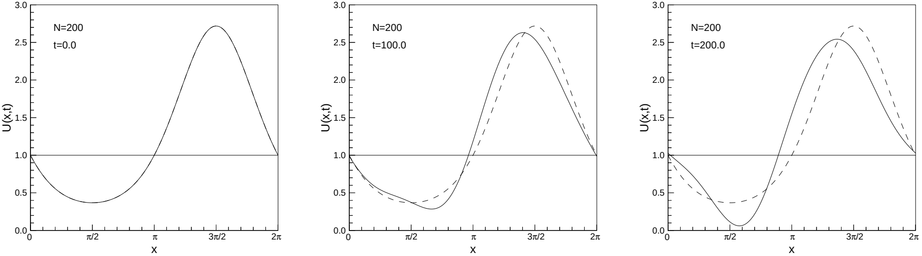

- Wave propagation with spectral method:

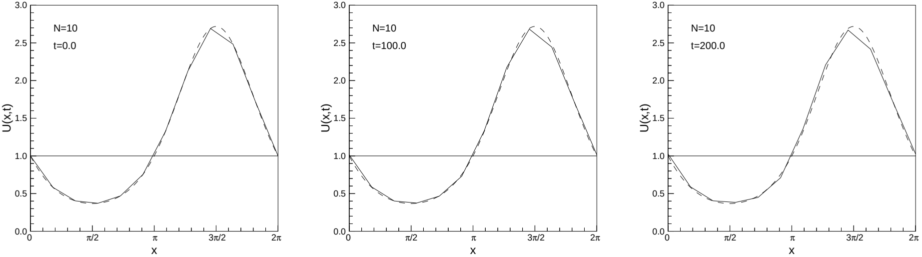

Figures from Hesthaven, Gottlieb, & Gottlieb (2007).

Moving Black Holes in a Spectral Code

- Spectral: Excision boundary is a smooth analytic surface.

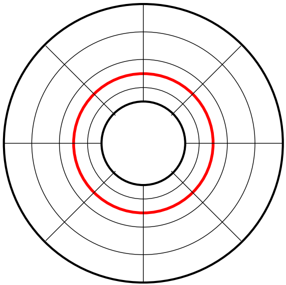

Moving Black Holes in a Spectral Code

- Spectral: Excision boundary is a smooth analytic surface.
  - Cannot add/remove individual grid points.

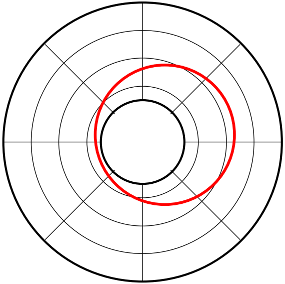

Moving Black Holes in a Spectral Code

- Spectral: Excision boundary is a smooth analytic surface.
  - Cannot add/remove individual grid points.
- Straightforward method: re-grid when holes move too far.

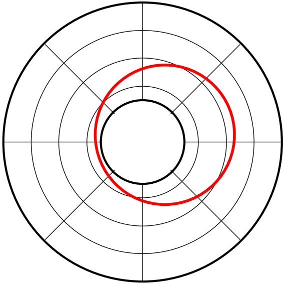

Moving Black Holes in a Spectral Code

- Spectral: Excision boundary is a smooth analytic surface.
  - Cannot add/remove individual grid points.
- Straightforward method: re-grid when holes move too far.

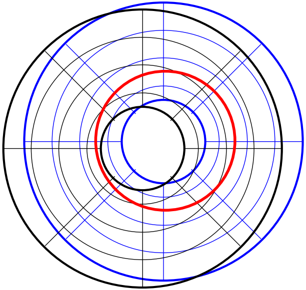

Moving Black Holes in a Spectral Code

- Spectral: Excision boundary is a smooth analytic surface.
  - Cannot add/remove individual grid points.
- Straightforward method: re-grid when holes move too far.

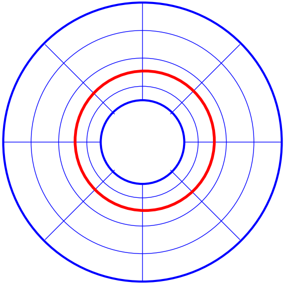

Moving Black Holes in a Spectral Code

- Spectral: Excision boundary is a smooth analytic surface.
  - Cannot add/remove individual grid points.
- Straightforward method: re-grid when holes move too far.
- Problems:
  - Re-gridding/interpolation is expensive.

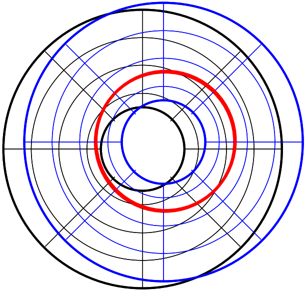

Moving Black Holes in a Spectral Code

- Spectral: Excision boundary is a smooth analytic surface.
  - Cannot add/remove individual grid points.
- Straightforward method: re-grid when holes move too far.
- Problems:
  - Re-gridding/interpolation is expensive.
  - Difficult to get smooth extrapolation at trailing edge of horizon.

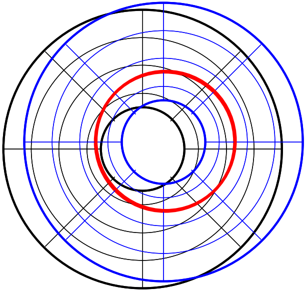

Moving Black Holes in a Spectral Code

- Spectral: Excision boundary is a smooth analytic surface.
  - Cannot add/remove individual grid points.
- Straightforward method: re-grid when holes move too far.
- Problems:
  - Re-gridding/interpolation is expensive.
  - Difficult to get smooth extrapolation at trailing edge of horizon.
  - Causality trouble at leading edge of horizon.

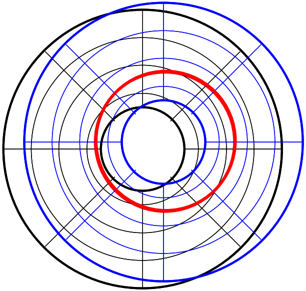

Moving Black Holes in a Spectral Code

- Spectral: Excision boundary is a smooth analytic surface.
  - Cannot add/remove individual grid points.
- Straightforward method: re-grid when holes move too far.
- Problems:
  - Re-gridding/interpolation is expensive.
  - Difficult to get smooth extrapolation at trailing edge of horizon.
  - Causality trouble at leading edge of horizon.

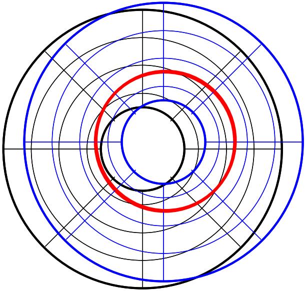

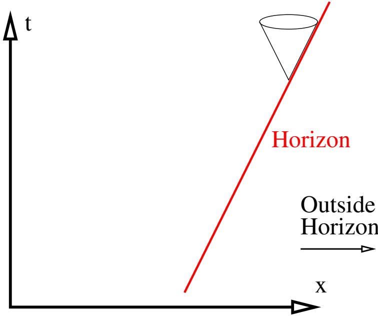

Moving Black Holes in a Spectral Code

- Spectral: Excision boundary is a smooth analytic surface.
  - Cannot add/remove individual grid points.
- Straightforward method: re-grid when holes move too far.
- Problems:
  - Re-gridding/interpolation is expensive.
  - Difficult to get smooth extrapolation at trailing edge of horizon.
  - Causality trouble at leading edge of horizon.

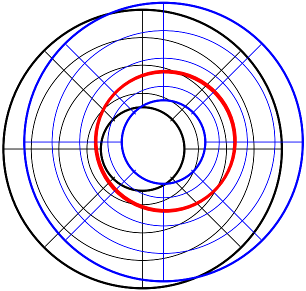

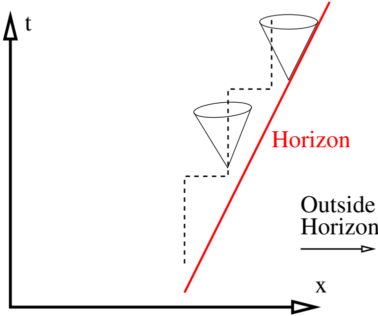

Moving Black Holes in a Spectral Code

- Spectral: Excision boundary is a smooth analytic surface.
  - Cannot add/remove individual grid points.
- Straightforward method: re-grid when holes move too far.
- Problems:
  - Re-gridding/interpolation is expensive.
  - Difficult to get smooth extrapolation at trailing edge of horizon.
  - Causality trouble at leading edge of horizon.
- Solution:

  Choose coordinates that smoothly track the location of the black hole.

  For a black hole binary this means using coordinates that rotate with respect to inertial frames at infinity.

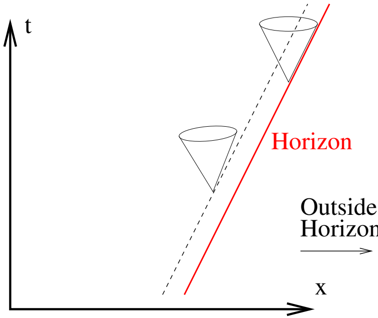

Horizon Tracking Coordinates

- Coordinates must be used that track the motions of the holes.
- This can be implemented by using a coordinate transformation from inertial coordinates, $\bar{x}^i$, to co-moving coordinates x^i, consisting of a rotation followed by an expansion:

$$\begin{aligned} x^i &= a(\bar{t})\, R^{(z)\,i}{}_j[\varphi(\bar{t})]\, R^{(y)\,j}{}_k[\xi(\bar{t})]\, \bar{x}^k, \\ t &= \bar{t}. \end{aligned}$$

- This transformation keeps the holes fixed in co-moving coordinates for suitably chosen $a(\bar{t})$, $\varphi(\bar{t})$ and $\xi(\bar{t})$.
- Motions of the holes are not known *a priori*, so $a(\bar{t})$, $\varphi(\bar{t})$, and $\xi(\bar{t})$ must be chosen dynamically and adaptively.
- A simple feedback-control system has been used to choose $a(\bar{t})$, $\varphi(\bar{t})$ and $\xi(\bar{t})$ by fixing the black-hole positions, even in evolutions with precession.

Evolving Black Holes in Rotating Frames

- Coordinates that rotate with respect to the inertial frames at infinity are needed to track the horizons of orbiting black holes.
- Evolutions of Schwarzschild in rotating coordinates are unstable.

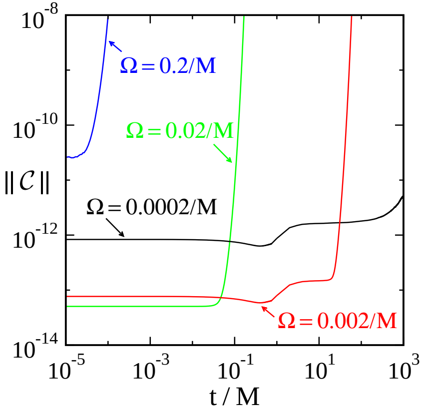

- Evolutions shown use a computational domain that extends to $r = 1000M$.
- Angular velocity needed to track the horizons of an equal mass binary at merger is about $\Omega \approx 0.2/M$.
- Problem caused by asymptotic behavior of metric in rotating coordinates: $\psi_{tt} \sim \rho^2\Omega^2$, $\psi_{ti} \sim \rho\Omega$, $\psi_{ij} \sim 1$.

Dual-Coordinate-Frame Evolutions

- Evolve inertial frame components of tensors using a rotating frame coordinate grid.

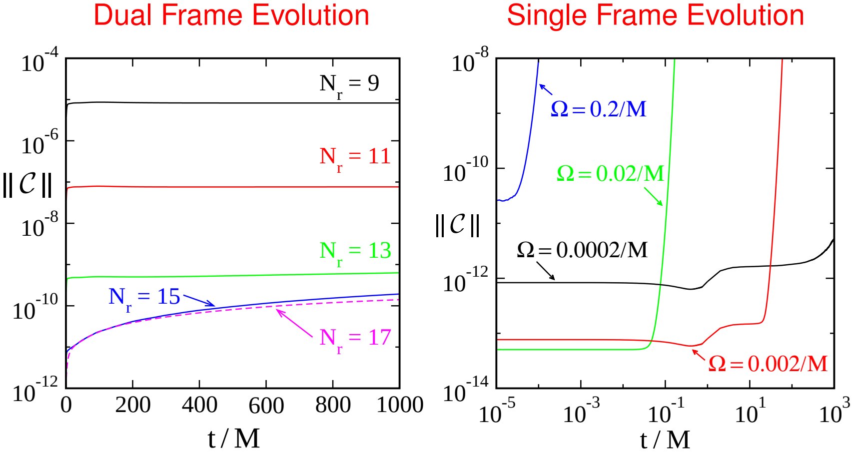

- Dual-frame evolution shown here uses a comoving frame with $\Omega = 0.2/M$ on a domain with outer radius $r = 1000M$.

Horizon Distortion Maps

- Tidal deformation, along with kinematic and gauge effects cause the shapes of the black holes to deform:

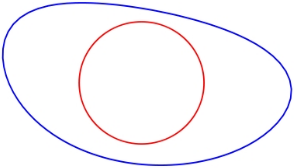

Horizon Distortion Maps

- Tidal deformation, along with kinematic and gauge effects cause the shapes of the black holes to deform:

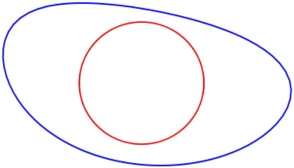

- If the holes become significantly distorted – relative to the spherical excision surface – bad things happen:
  - Some points on the excision boundary are much deeper inside the singular black hole interior. Numerical errors and constraint violations are largest there, sometimes leading to instabilities.

Horizon Distortion Maps

- Tidal deformation, along with kinematic and gauge effects cause the shapes of the black holes to deform:

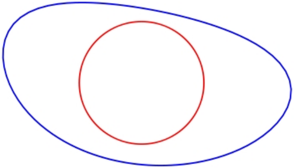

- If the holes become significantly distorted – relative to the spherical excision surface – bad things happen:
  - Some points on the excision boundary are much deeper inside the singular black hole interior. Numerical errors and constraint violations are largest there, sometimes leading to instabilities.
  - When the horizons move relative to the excision boundary points, the excision boundary can become timelike, and boundary conditions are then needed there.

Horizon Distortion Maps II

- Adjust the placement of grid points near each black hole using a horizon distortion map that connects grid coordinates x^i to points in the black-hole rest frame $\tilde{x}^i$:

$$\tilde{\theta}_A = \theta_A, \qquad \tilde{\varphi}_A = \varphi_A,$$

$$\tilde{r}_A = r_A - f_A(r_A, \theta_A, \varphi_A) \sum_{\ell=0}^{L} \sum_{m=-\ell}^{\ell} \lambda_A^{\ell m}(t) Y_{\ell m}(\theta_A, \varphi_A).$$

- Adjust the coefficients $\lambda_A^{\ell m}(t)$ using a feedback-control system to keep the excision surface the same shape and slightly smaller than the horizon, and to keep the characteristic speeds from becoming ingoing.
- Choose f_A to scale linearly from $f_A = 1$ on the excision boundary, to $f_A = 0$ on cut sphere.

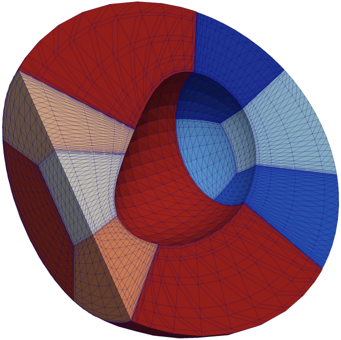

Spectral AMR (As Implemented by Belá Szilágyi)

- Measure the truncation error in each sub-domain by comparing the power in the lowest spectral coefficients with the highest:

$$\mathcal{E} = \frac{\text{Power in high order modes}}{\text{Power in low order modes}}.$$

- Add more spectral coefficients when/where $\mathcal{E}$ gets too large.
- Remove spectral coefficients when/where $\mathcal{E}$ gets too small.

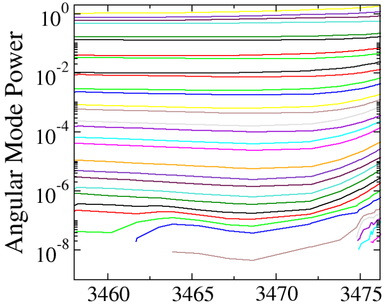

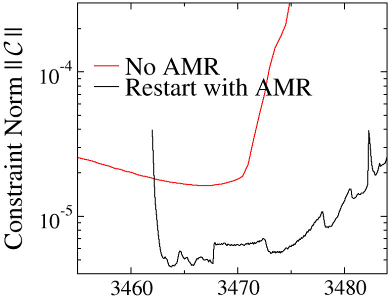

- High spin evolutions of Lovelace, Scheel, & Szilágyi (2010) required AMR to achieve successful merger.

Caltech/Cornell Spectral Einstein Code (SpEC):

- Multi-domain pseudo-spectral evolution code.

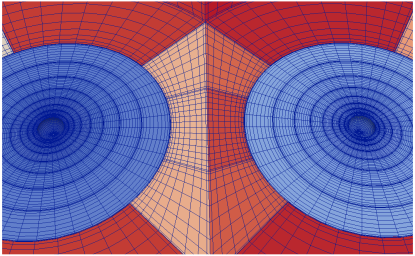
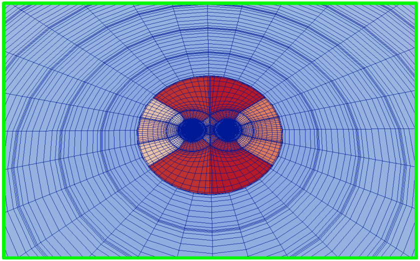

Lovelace, Scheel, & Szilágyi (2010) high spin evolution grids.

- Constraint damped “generalized harmonic” Einstein equations:
$$\psi^{cd}\partial_c\partial_d\psi_{ab} = F_{ab}(\psi, \partial\psi).$$
- Dual frame evolutions with horizon tracking and distortion maps.
- Spectral AMR.
- Constraint-preserving, physical and gauge boundary conditions.

Outline of Talk:

- Fundamental Einstein Equation Issues.
  - How Gauge is Specified.
  - Making Einstein's Equation Hyperbolic.
  - Constraints and Constraint Damping.
  - Good Gauge Conditions.
- Numerical Method Issues.
  - Solving Evolution Equations.
  - Horizon Tracking Coordinates.
  - Dual-Frame Evolution.
  - Horizon Distortion Maps.
  - Spectral AMR.
- A Sample of Recent BBH Evolution Results.
  - Post-Merger Recoils.
  - Accurate Long Waveforms.
  - Very High Mass Ratios.
  - Very High Spins.

Post-Merger Recoils

- Mergers of asymmetric binaries (unequal masses and/or unequal or nonaligned spins) emit gravitational waves asymmetrically.
- Resulting single black hole has a "kick" velocity relative to the pre-merger center of mass.
- Kicks in asymmetric non-spinning binaries first studied by the Penn State and Jena groups (2006-07).
- Figure from González, Sperhake, and Brügmann (2009).

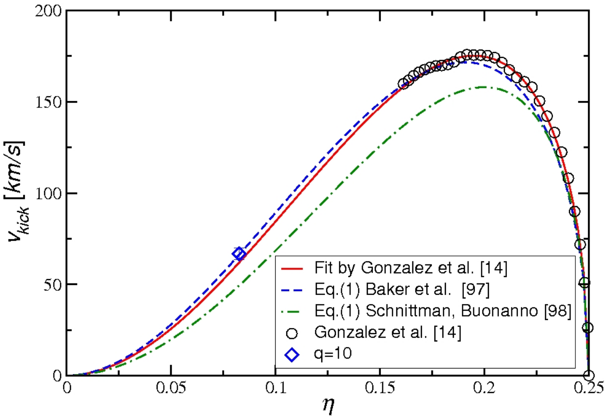

Post-Merger Recoils with Spin

- Mergers of spinning black-hole binaries can result in large recoils.
- Maximum kicks are produced by mergers with anti-parallel spins tangent to the orbital plane.

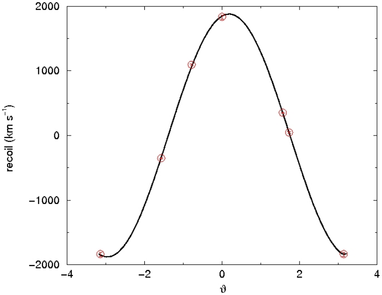

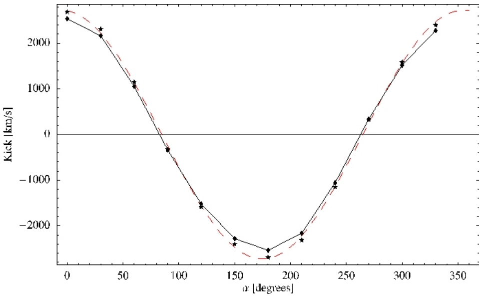

- Campanelli, et al. (2007): Kick velocities as function of orbital phase for black holes with spin $\chi \approx 0.5$.
- Brügmann, et al. (2007): Analogous results for black holes with spin $\chi \approx 0.72$.
- Maximum kick velocity $v_{\max} \approx 4000$ km/s predicted for maximum spin, $\chi_1 = -\chi_2 = 1$, equal-mass black-hole mergers.

Accurate Long Waveform Simulations

- Numerical waveforms must be accurate enough to satisfy LIGO's data analysis requiements.
- Numerical waveforms must be long enough to allow matching onto PN or EOB waveforms without loss of accuracy.

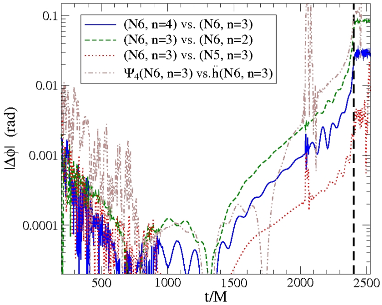

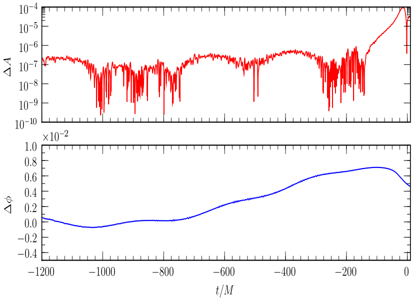

- Recent Caltech/Cornell: accurate aligned-spin waveforms, Pan, et al. (2010).
- Recent AEI/LSU: accurate non-spinning waveforms, Pollney, et al. (2010).

Very High Mass Ratios

- Numerical simulation of high mass-ratio binaries is very difficult:
  - Very high spatial resolution needed near the smaller black hole.
  - Time steps set by the smallest spatial resolution (explicit schemes).
  - Radiation reaction timescale proportional to mass ratio $M/m \gg 1$, so many orbits required to achieve merger.
- Jena group performed $M/m \approx 10$ simulations (2009), RIT group recently announced $M/m \approx 100$ simulations (2010).

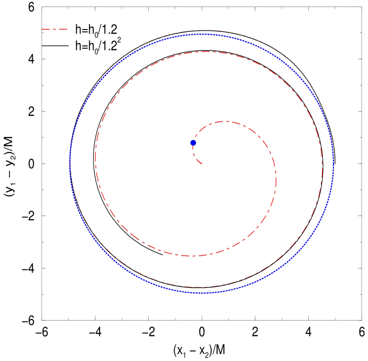

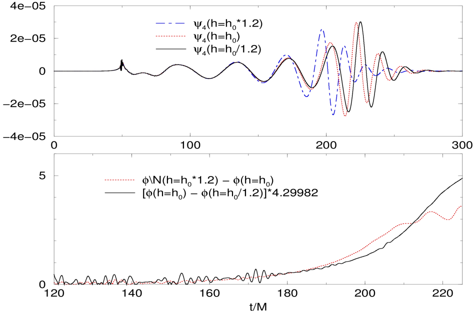

High Spin Evolutions

- Lovelace, Scheel, & Szilágyi (2010) use high spin conformal initial data from superimposed boosted Kerr-Schild black holes.
- Spins $\chi \approx 0.95$ anti-aligned with orbital angular momentum.
- Evolve through 12.5 orbits, merger, and ringdown.
- High accuracy gravitational waveform extracted.
- Lovelace, et al. Spin Movie.

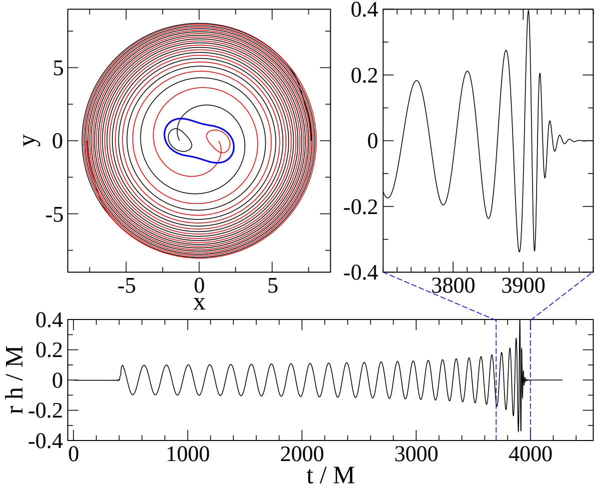

Summary

- The NR community has made great progress on a number of fundamental problems:
  - Numerous hyperbolic representations of GR: BSSN and GH and ...
  - Constraint violating instabilities controlled.
  - Inner boundary problems controlled: moving puncture or excision.
  - Effective gauge conditions: 1+log, Γ-driver, damped harmonic, ...
  - Effective outer boundary conditions: outgoing physical gw, constraint preserving, ...
- Great progress on numerical and code development issues:
  - Higher order FD and spectral numerical methods.
  - AMR for FD and spectral methods.
  - Moving puncture methods.
  - Excision plus dual-frame dynamical horizon-tracking coordinates using feedback-control.
- Interesting physical results:
  - Large astrophysically interesting post-merger kicks.
  - Accurate emperical post-merger parameter estimation.
  - Long acccurate waveforms for GW data analysis.